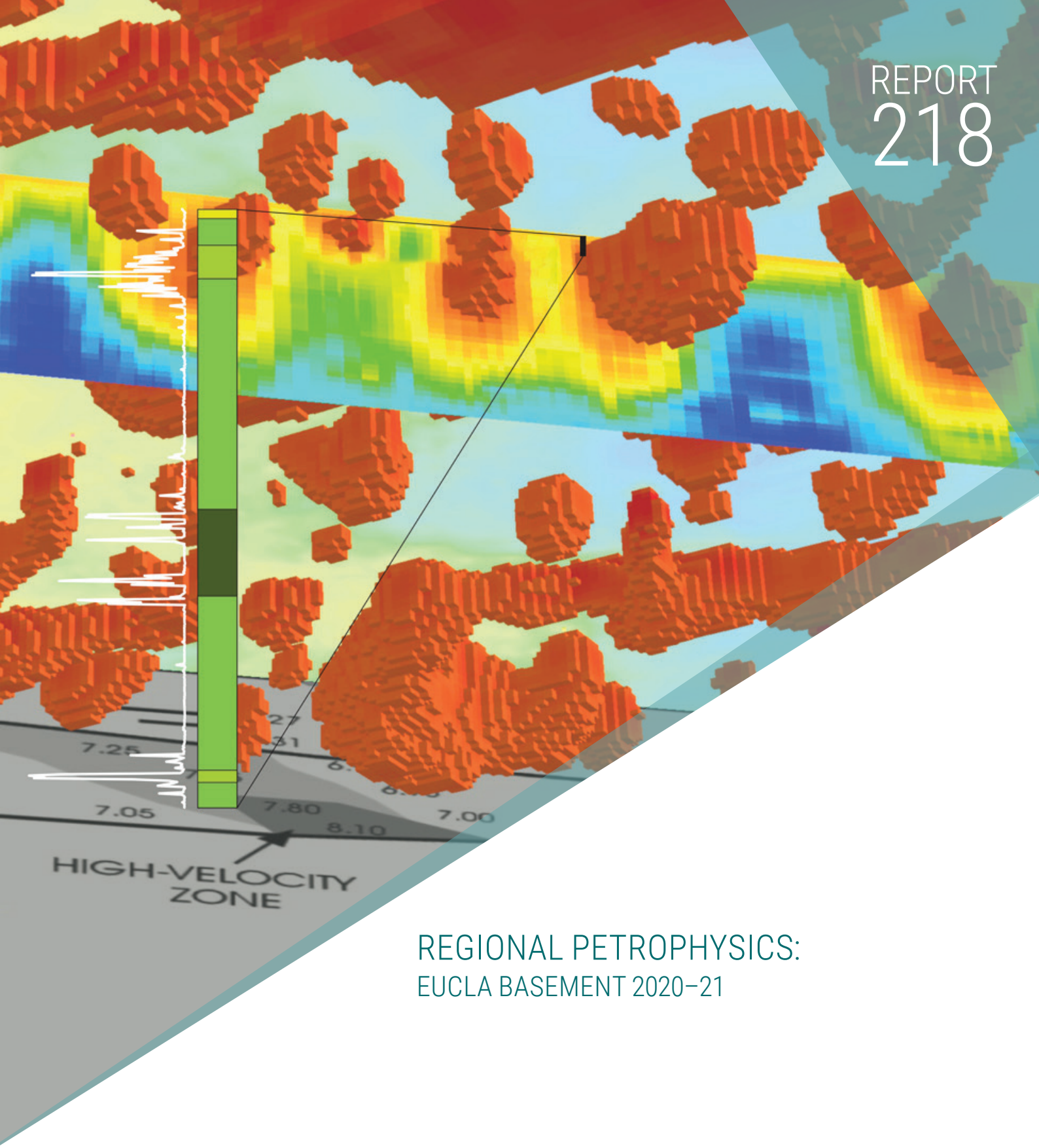

REPORT
218

REGIONAL PETROPHYSICS:
EUCLA BASEMENT 2020–21

by
M Markoski, J Trunfull and B Bourne

Government of **Western Australia**
Department of **Mines, Industry Regulation and Safety**

Geological Survey of Western Australia

Government of **Western Australia**
Department of **Mines, Industry Regulation and Safety**

REPORT 218

REGIONAL PETROPHYSICS: EUCLA BASEMENT 2020–21

by
M Markoski*, J Trunfull* and B Bourne*

* Terra Petrophysics Pty Ltd, Unit 5/51 Forsyth Street, O'Connor Western Australia 6163

PERTH 2021

Geological Survey of Western Australia

MINISTER FOR MINES AND PETROLEUM
Hon Bill Johnston MLA

DIRECTOR GENERAL, DEPARTMENT OF MINES, INDUSTRY REGULATION AND SAFETY
Richard Sellers

EXECUTIVE DIRECTOR, GEOLOGICAL SURVEY AND RESOURCE STRATEGY
Jeff Haworth

REFERENCE
The recommended reference for this publication is:
Markoski, M, Trunfull, J and Bourne, B 2021, Regional petrophysics: Eucla basement 2020–21: Geological Survey of Western Australia, Report 218, 25p.

ISBN 978-1-74168-938-9
ISSN 1834-2280

A catalogue record for this book is available from the National Library of Australia

Grid references in this publication refer to the Geocentric Datum of Australia 1994 (GDA94). Locations mentioned in the text are referenced using Map Grid Australia (MGA) coordinates, Zones 51 and 52. All locations are quoted to at least the nearest 100 m.

About this publication
Petrophysical measurements were made by Terra Petrophysics Pty Ltd, as a collaborative research agreement with the Geological Survey of Western Australia, funded by the Exploration Incentive Scheme.

Published 2021 by the Geological Survey of Western Australia
This Report is published in digital format (PDF) and is available online at <www.dmirs.wa.gov.au/GSWApublications>.

Further details of geoscience publications are available from:
Information Centre
Department of Mines, Industry Regulation and Safety
100 Plain Street
EAST PERTH WESTERN AUSTRALIA 6004
Telephone: +61 8 9222 3459 Email: publications@dmirs.wa.gov.au
www.dmirs.wa.gov.au/GSWApublications

Cover photograph: Down core petrophysical data shown in relation to crustal scale density and velocity models

Introduction

The Geological Survey of Western Australia's (GSWA) regional petrophysics project aims to provide a statewide petrophysical dataset that can be used in the planning and interpretation of geophysical data. This project commenced in 2020–21, in collaboration with Terra Petrophysics, and is funded by the Exploration Incentive Scheme (EIS).

In 2020–21, this project acquired petrophysical data from diamond drillcores, largely EIS co-funded drillcores but also including core loaned and donated by companies, in the Paterson Orogen (n = 274), West Arunta (n = 975), Eucla basement (n = 93), Yamarna (n = 346) and Kalgoorlie Terranes (n = 1651). All the drillcore sampled for petrophysics have accompanying HyLogger data (or will have) and most have open-file company assay data, available from the Mineral Exploration reports database (WAMEX). For each project, a report and datasheet have been produced by Terra Petrophysics. The report contains a description of the methods, a first-pass analysis of the data, a summary of the petrophysical measurements (Appendix 1) and a photo of each sample (Appendix 2). The complete dataset of petrophysical measurements, lithological information and supplementary material can be found in the datasheets, which are available in MAGIX and GeoVIEW.WA.

This report describes the petrophysical data acquired from the Eucla basement in 2020–21 (Fig. 1; Table 1). The report and datasheet are also available as a downloadable zip file (http://geodownloads.dmp.wa.gov.au/downloads/geophysics/72014.zip).

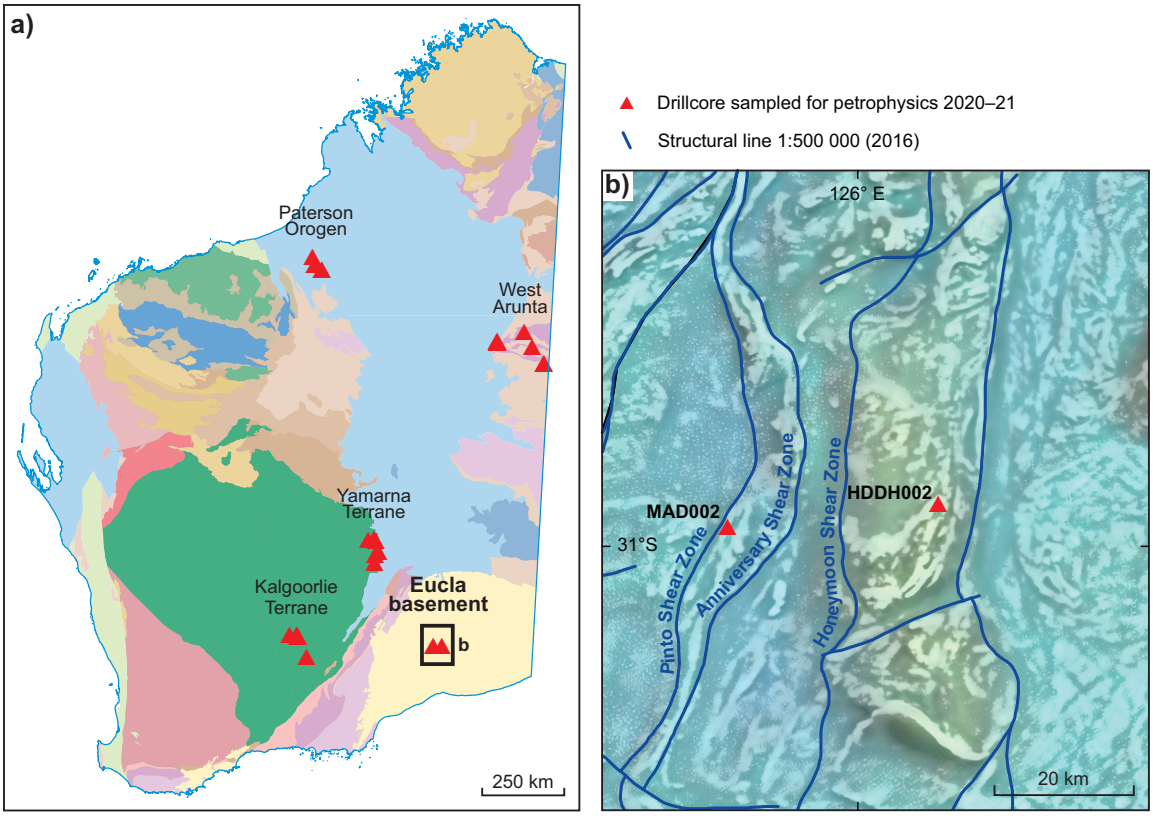

Figure 1. Drillcores sampled for petrophysical data in 2020–21: a) all drillcores, shown on tectonic units map (2016); b) Eucla basement drillcores, shown on Bouguer gravity data (colour) draped with 1VD total magnetic intensity data (grey scale)

Table 1. Eucla basement drillcores sampled for petrophysical data in 2020–21

Drillhole	Datum	UTM Zone	Easting	Northing	Azimuth	Dip	Depth (m)	Petrophysical samples	EIS
HDDH002	GDA 94	52	223271	6572880	315	–70	483.7	42	Yes
MAD002	GDA 94	51	770428	6569645	280	–80	591.6	51	Stratigraphic

LIB75-2 01.09.21

TERRA PETROPHYSICS PTY. LTD.

(ABN 71 613 484 807)

GEOLOGICAL SURVEY OF WESTERN AUSTRALIA

EUCLA PROJECT

WESTERN AUSTRALIA

TECHNICAL REPORT NO. 20_032

DATUM / PROJECTION
GDA94 / MGA Zone 51/52

DISTRIBUTION

1. GSWA – Lucy Brisbout
2. Terra Petrophysics – Barry Bourne
3. Terra Petrophysics – Jarrad Trunfull

Mila Markoski
Geoscientist
February 2021

TERRA PETROPHYSICS

TABLE OF CONTENTS

1. INTRODUCTION

Terra Petrophysics have performed petrophysical analysis of 93 rock (drill core) samples from the Eucla province of Western Australia. These samples have been selected and provided by GSWA in a joint initiative with Terra Petrophysics to develop an understanding of physical properties of rocks in the region and to assist with the interpretation of geophysical field data. Petrophysical analysis includes measurement of the following physical properties:

- Induced Polarisation (Chargeability) and Galvanic Resistivity
- Inductive Conductivity
- Magnetic Susceptibility
- Remanent Magnetisation; the ratio of induced- to remanent-magnetisation intensity of the sample (known as the Koenigsberger Ratio, Q), as well as an estimate of the total remanent vector (relative to drill hole).
- Dry Bulk Density
- Apparent Porosity
- P-wave Sonic Velocity

During analysis, Terra Petrophysics utilise standards and reference samples to ensure precision and accuracy.

2. PETROPHYSICS

2.1 Sample Preparation

Samples for physical property measurements should be selected for quality and representation of lithology and alteration. Terra recommends samples of 10 to 15 cm length. In this study, all samples were of adequate size and quality. The size and shape of the sample need to be determined for most physical property measurements (e.g., geometric and core size correction factors). All samples are returned to the client after analysis.

Samples are photographed and marked with Terra Petrophysics sample numbers. All samples should be accompanied by a project name, a brief description of each sample as well as ancillary data (geological logging, assays), requested physical property procedures and final disposal requirement for the samples.

Physical property determinations are non-destructive procedures; however, some measurements require the sample to have flat/square edges which requires them to be cut using a rock saw. In addition, samples are required to be submerged in water for 24 hours for measurement. Strongly weathered and friable samples can be damaged by the soaking process, and each sample is inspected prior and the process modified (if required) to ensure that minimal damage occurs.

2.2 Inductive Conductivity

The inductive conductivity measurement is made in the frequency domain at 10,000 Hz via an external magnetic field inducing a small current in the sample. The measurement is most influenced by sample material at the receiver coil and within a 10 cm radius from the centre of the sample.

Inductive conductivity is calculated from the difference in amplitude between the sample and free air measurements. Resulting data are presented in S/m, and the limits of detectability are 0.1 S/m (lower) and 100,000 S/m (upper). Several inductive conductivity measurements will be made at different points and at different angles on the sample.

2.3 Induced Polarisation and Resistivity

The apparent resistivity and induced polarisation (or chargeability) determinations are measured in time domain. The resistivity and chargeability values are measured by passing a constant current through the sample and then switching it on and off at 2 second intervals. Whilst current is flowing through the sample, the resistivity (Ωm) is calculated. When the current is switched off, the voltage across the sample decays to zero and this decay curve is measured. The induced polarisation (mV/V) is calculated between 450 and 1100 milliseconds after turn off (referred to as the Newmont Standard). Resistivity and induced polarisation values are stacked and averaged a minimum of 10 times for one reading. Terra provide the averaged results over several readings.

Some samples (for example, silica rich samples) can be so resistive as to act dielectric. Charged particles do not flow through the sample as if it were conductive, but instead are shifted slightly from their original position due to the potential difference. When the current is switched off, the charged particles slowly relax to their original state and thus generate a decay signal, which is integrated into a chargeability value. Therefore, some very resistive samples can appear to be more chargeable than would be recognised by a field IP survey.

2.4 Wet/Dry Bulk Density and Porosity

The density determinations are calculated using Archimedes' principle. Dry bulk densities are determined by dry weight divided by the buoyancy determined volume of each sample. Porosities are calculated from water saturated weights, dry weights, and the buoyancy-determined volume. All sample are soaked for at least 24 hours (where possible) after dry weights are measured.

The accuracy of the buoyancy technique of density measurement is 0.01 grams per cubic centimetre (g/cm^3). The results of the laboratory density determinations are reported in grams per cubic centimetre. Density measurements can be made on grab samples or drill core. Very large or heavy samples (>1 kg) require coring or breaking prior to the density determination.

2.5 Magnetic Susceptibility and Remanence

Magnetic susceptibility is measured by using a magnetic susceptibility meter to apply an external magnetic field to the sample at an operating frequency of 8 kHz. Magnetic susceptibility is calculated from the frequency difference between the sample and free air measurements. The limits of detectability are approximately 1×10^{-7} SI units and resulting data is presented in SI ($\times 10^{-3}$) units. The measurement is most influenced by sample material at the receiver coil and within a 10 cm radius from the centre of the sample. Magnetic susceptibility measurements can be made on core, hand and surface samples.

For magnetic samples ($>5\times 10^{-3}$ SI) the magnetic remanence can be measured. The measurement of remanence (J_{rem}) in the field and the ratio of remanence to the induced magnetisation (J_{rem}/J_{ind} = Q) has in the past been problematic. The induced magnetisation can be estimated using the susceptibility (k, where J_{ind} = kH and typically H = 40-50 Am^{-1}) which can be measured using a handheld meter, but magnetic remanence is more difficult.

A recent development in field instrumentation uses a miniature fluxgate magnetometer and a pendulum arrangement in which a magnetic rock may be swung generating a transient signal at the fluxgate which is converted to a magnetic moment and magnetisation.

2.6 Velocity

Terra Petrophysics can acquire P-wave velocity measurements on samples with a minimum length of 15 centimetres. Measurements are taken at 50,000 Hz. The velocity measurement limits of detectability are 1500 m/s (lower) to 9999 m/s (upper).

3. RESULTS

A total of 93 samples have undergone petrophysical analysis, and a results table is included as Appendix 1. Each sample is assigned a Terra ID and photographs of the samples have been included in Appendix 2. Raw data for the induced polarisation and resistivity measurements are included in the attached spreadsheet. Various plots of petrophysical data are given in Figures 2 to 13.

A legend corresponding to Figure 2 to Figure 13 is given in Figure 1. The data points have been represented using three different categories: Ni content (ppm), which is represented by cool-warm colours; Cu content (ppm), which is represented by symbol size; and lithology, which is represented by shape. Black symbols have not been assayed for Ni or Cu.

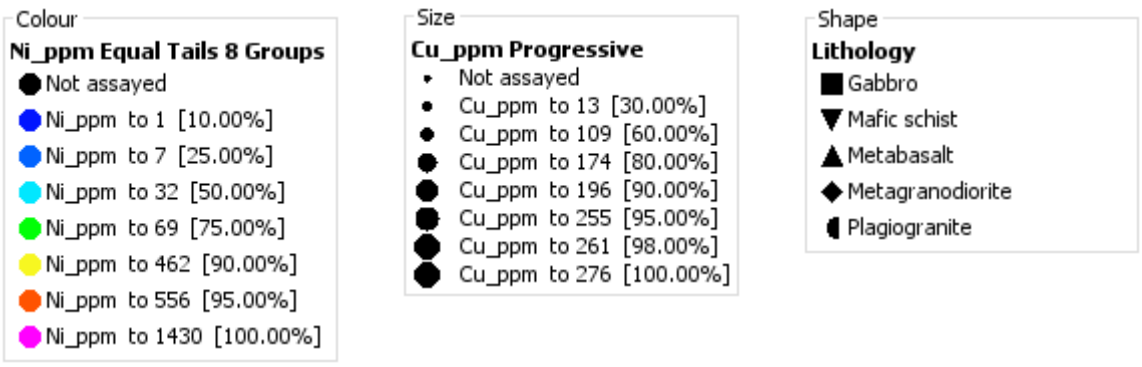

Figure 1. Legend corresponding to Figures 2 to 13.

Figure 2 displays dry bulk density against magnetic susceptibility. The dry bulk density for the sample suite ranges from 2.65 to 3.24 g/cm^3 and the magnetic susceptibility ranges from 0.359 to 372 ($\times 10^{-3}$) SI.

It can be observed that mafic lithologies (predominantly gabbro, mafic schist and metabasalt), which also contain elevated levels of Cu and Ni, correspond to higher densities (>3.00 g/cm^3), but there is no obvious correlation with magnetic susceptibility. Samples with more elevated Ni are not observed to have a strong magnetic susceptibility response either, with these samples (mostly mafic schists) showing between 0.9 and 2.8 ($\times 10^{-3}$) SI, and with a density between 2.9 and 3.15 g/cm^3 (circled in red). Note that black points signify no assay information.

A diagram to convert magnetic susceptibility to theoretical magnetic mineral content is given in Figure 3 (from Emerson, 1997); using Figure 3, sample 20TR2334 (which has a magnetic susceptibility of 0.372 SI) could be estimated to contain roughly 10% magnetite (as represented by the red line). Figure 4 shows dry bulk density ranges for a range of common rock types (from Emerson, 1990).

The highest Ni content of all samples was 1430 ppm, from a mafic schist (20TR2308). This corresponded to a magnetic susceptibility of 2.32 $\times 10^{-3}$ SI and a dry bulk density of 3.24 g/cm^3.

The highest Cu content of all samples was 276 ppm, from a gabbro (20TR2355). This corresponded to a magnetic susceptibility of 70.387 $\times 10^{-3}$ SI and dry bulk density of 3.11 g/cm^3.

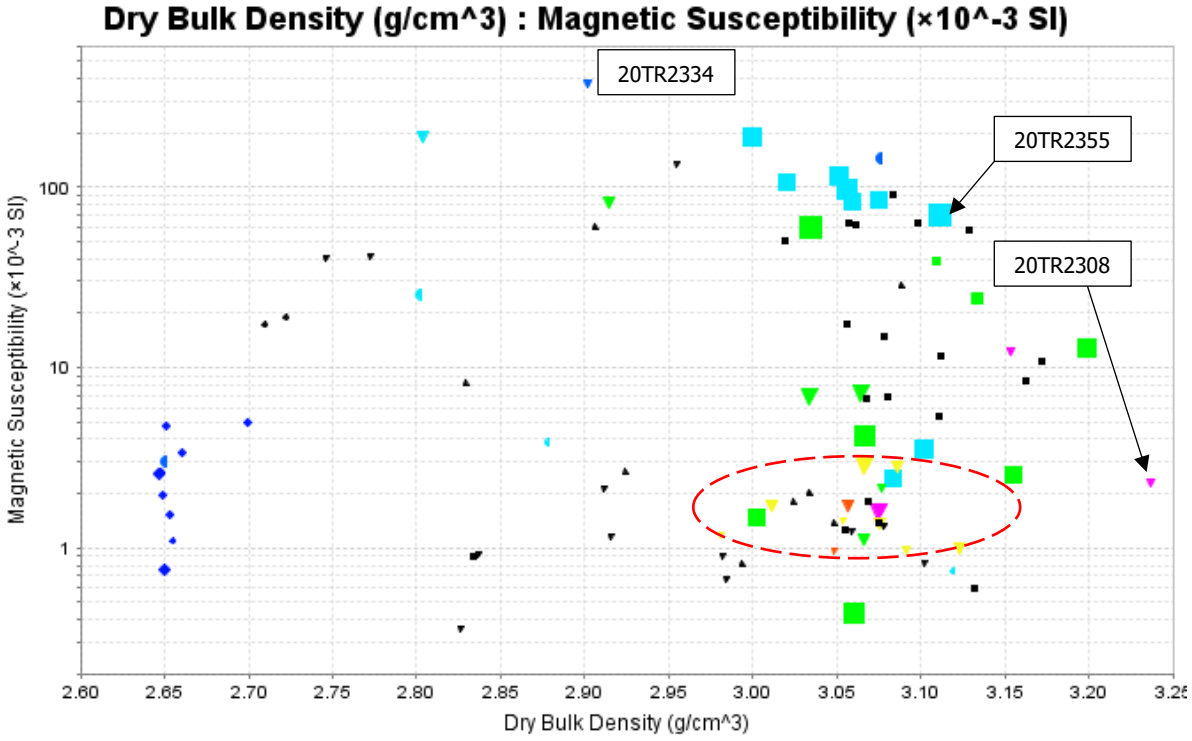

Figure 2. Cross-plot of dry bulk density against magnetic susceptibility.

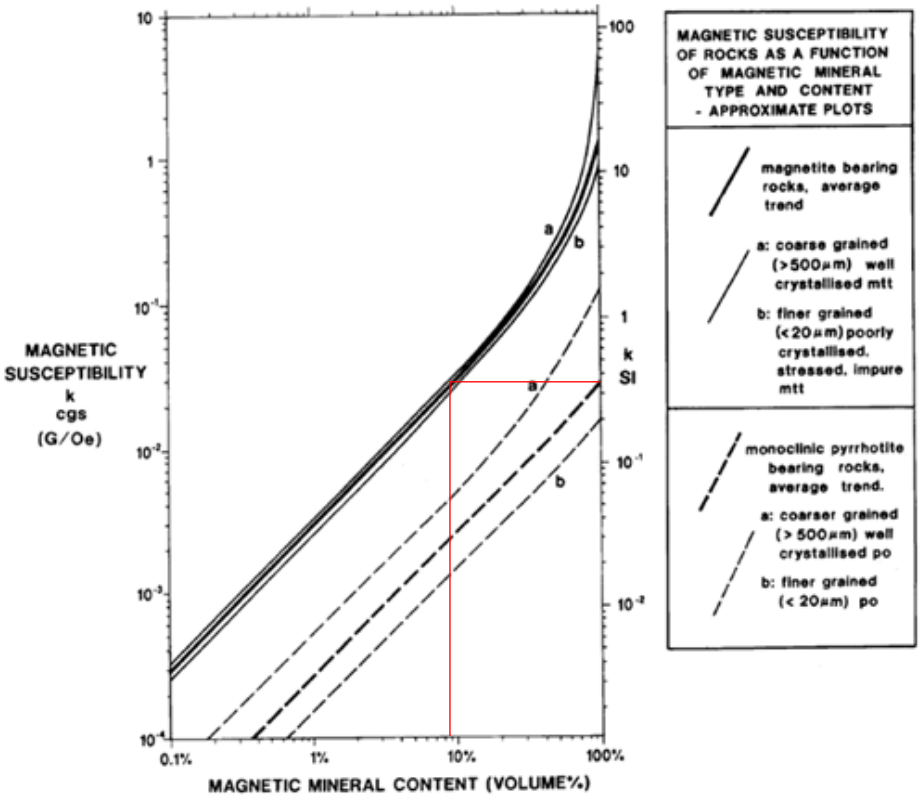

Figure 3. Theoretical magnetic mineral content (magnetite – solid lines; pyrrhotite – dashed lines) as a function of measured magnetic susceptibility (Emerson, 1997)

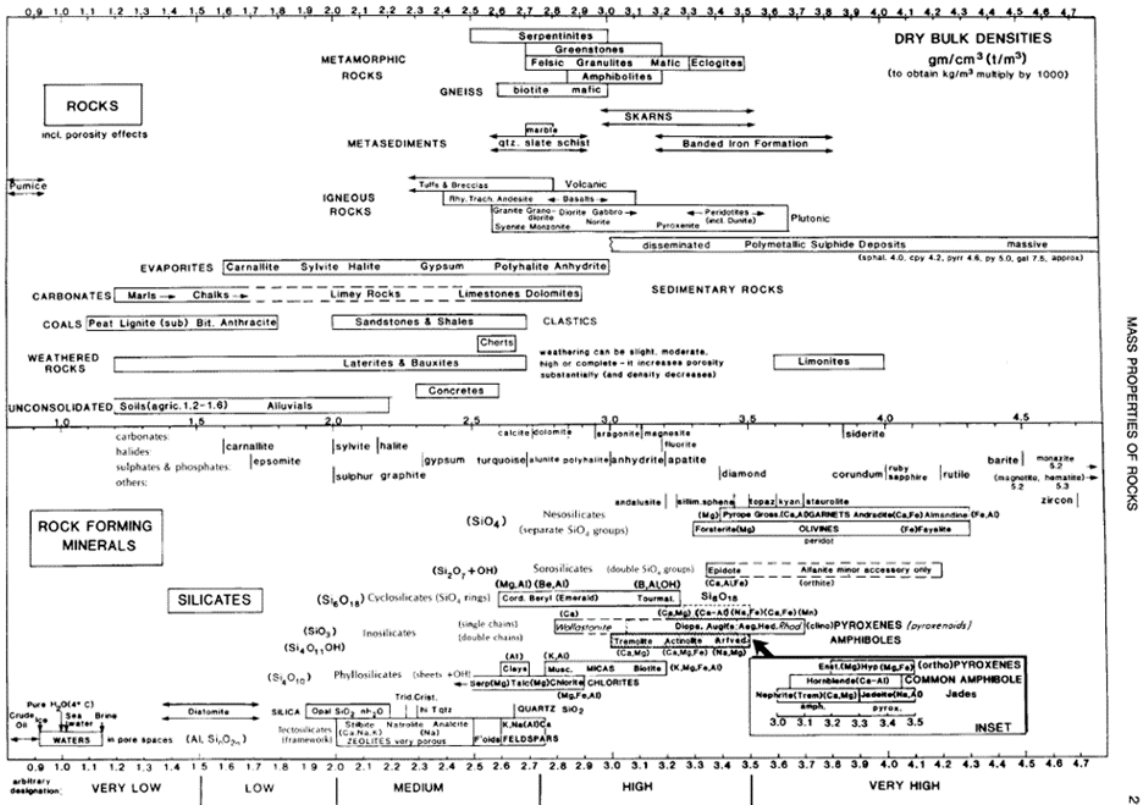

Figure 4. Dry bulk density ranges for common rock types (Emerson, 1990)

Figure 5 shows dry bulk density plotted against galvanic resistivity. The samples in this suite exhibit a large range of resistivity values, from 200 to over 1,000,000 Ωm. Dry bulk density data range from 2.65 and 3.24 g/cm^3.

The denser gabbro samples show a range of resistivity values (from 2832 Ωm to over 1,000,000 Ωm). The Ni-elevated mafic schists cluster around 3.00 to 3.15g/cm^3 and correspond to lower resistivities (<10,000 Ωm, circled in red), which could be due to the presence of sulphides.

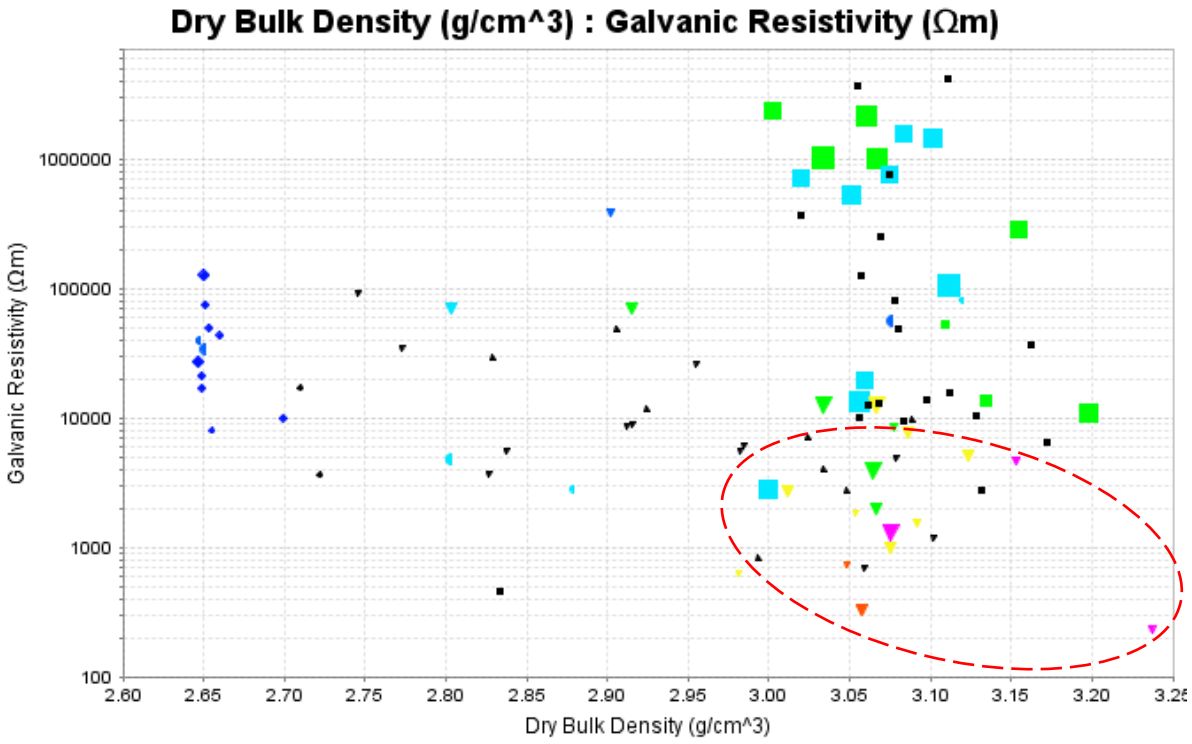

Figure 5. Cross-plot of dry bulk density against resistivity.

Figure 6 shows magnetic susceptibility plotted against galvanic resistivity. Magnetic susceptibility values range between 0.359 and 372 ($\times 10^{-3}$) SI, and resistivity values range from 200 to over 1,000,000 Ωm.

Four 'clusters' of data can be observed in this plot; a bulk trend that exhibits a positive correlation between magnetic susceptibility and resistivity (as indicated by the grey trendline), a cluster of mostly Cu-elevated gabbros with extremely high resistivity and low magnetic susceptibility values (circled in blue) that appears separate to a cluster of gabbro with a higher magnetic susceptibility (circled in green), and a cluster of Ni-elevated mafic schist samples that correspond to lower resistivity and magnetic susceptibility values (circled in red).

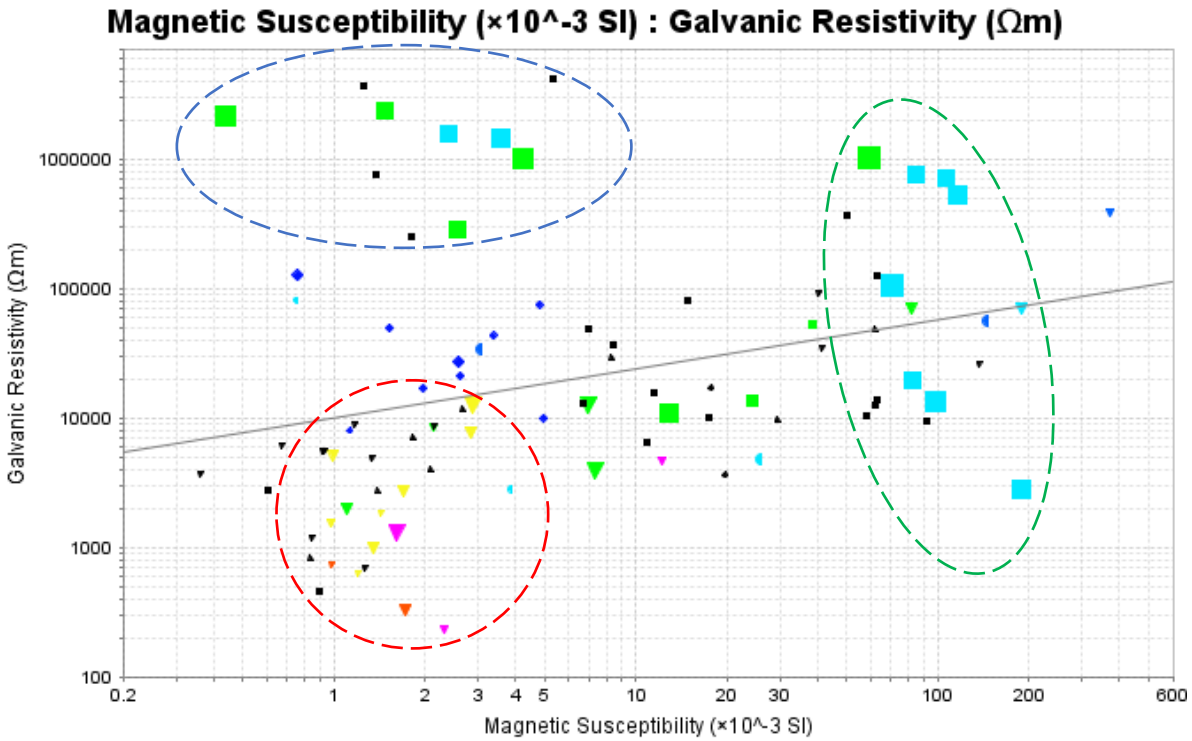

Figure 6. Cross-plot of magnetic susceptibility against resistivity.

Figure 7 shows a cross-plot of chargeability against galvanic resistivity. Chargeability values for the sample suite range between 2.2 and 85.2 mV/V.

Highly resistive samples in this dataset have exhibited the dielectric phenomenon (as explained in Section 2.3). This is illustrated by the red dashed line, where increasingly resistive samples also appear increasingly chargeable.

Separately to this effect, there appears to be three samples with distinctly high chargeability values (>70 mV/V); 20TR2301, 20TR2304 and 20TR2318. These samples appear to contain sulphides (although they have not been assayed).

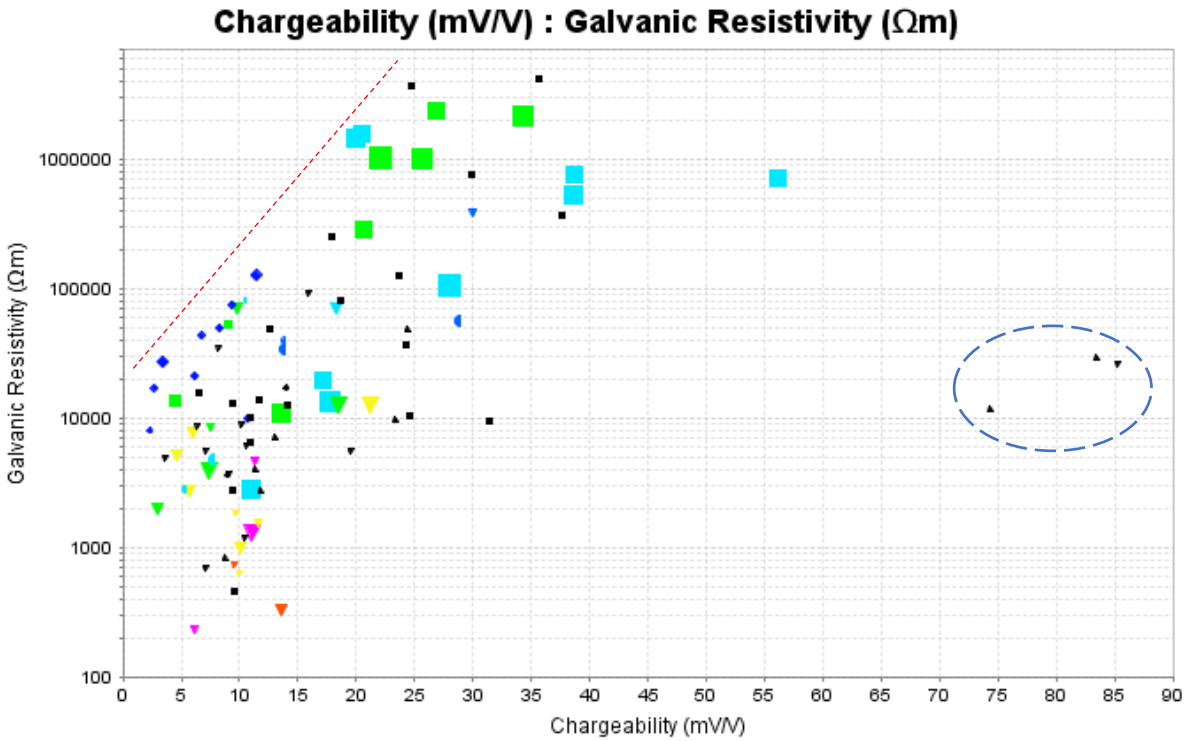

Figure 7. Cross-plot of chargeability against resistivity.

Figure 8 displays chargeability values plotted against magnetic susceptibility.

There appears to be no obvious correlation between the two properties. Mafic schists with elevated Ni appear to correspond to low magnetic susceptibility and chargeability values.

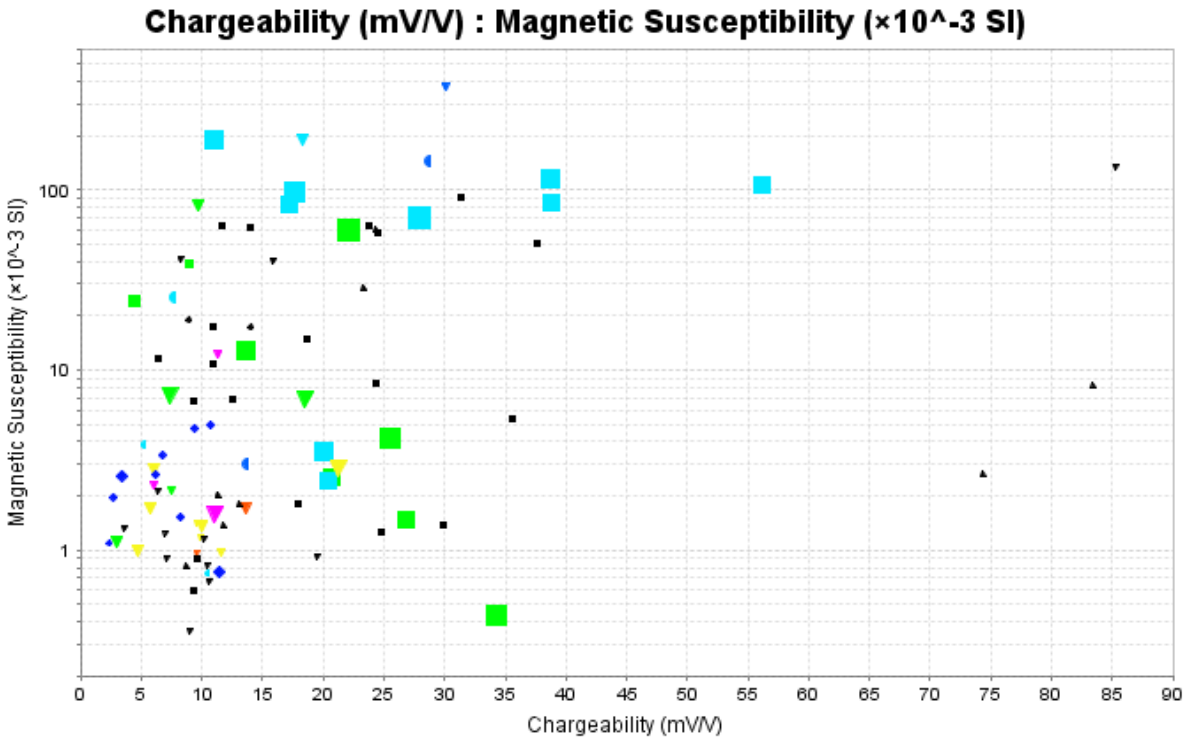

Figure 8. Cross-plot of chargeability against magnetic susceptibility.

Figure 9 displays inductive conductivity plotted against chargeability. Only samples with a non-zero conductivity values are displayed on the plot.

Chargeability of a material is dependent on 4 major factors: the degree of sulphide or metallic mineralisation, presence of clays, the pore-water salinity, and the overall tortuosity of the pore-space network within the rock. Both a high inductive conductivity and a high chargeability may be indicative of the presence of sulphides within the sample, although conductivity tends to better respond to massive (connected) sulphides, while chargeability responds better to disseminated (disconnected) sulphides.

Three samples showed a non-zero conductivity, and all had a conductivity value of less than 4 S/m. These correlate with non-significant chargeability values of <15 mV/V.

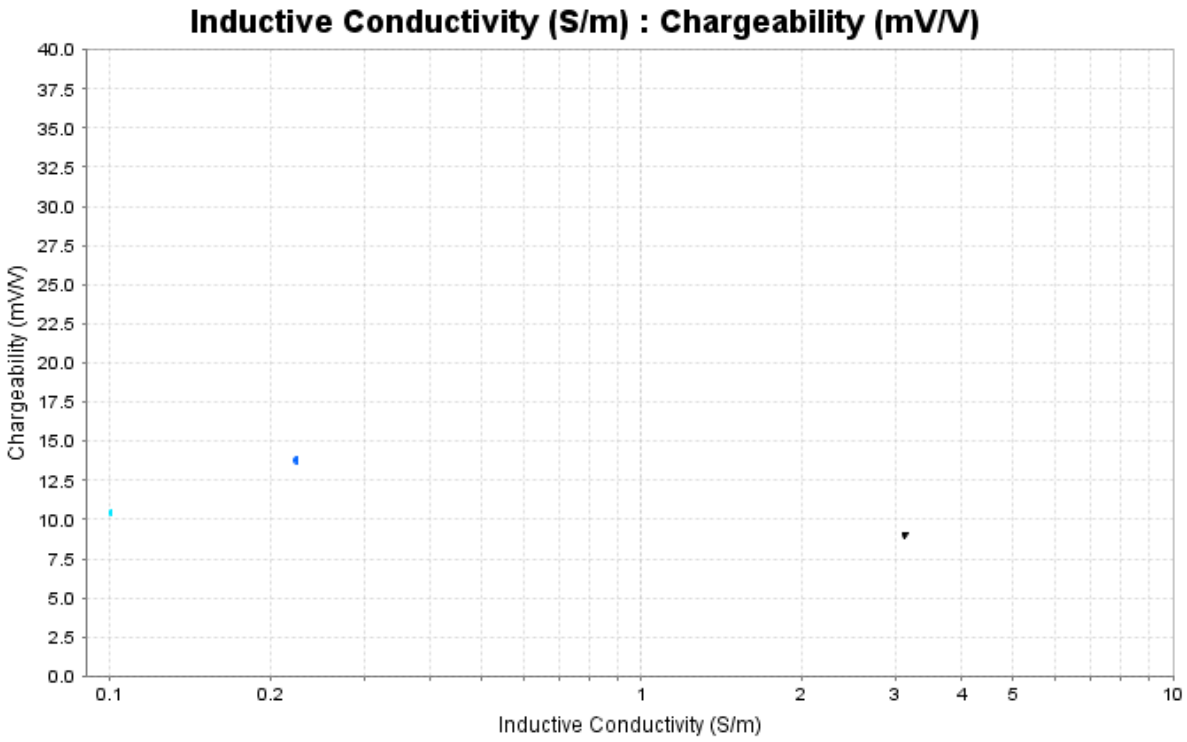

Figure 9. Cross-plot of inductive conductivity against chargeability.

Figure 10 plots the dry bulk density and apparent porosity of samples against known reference mineral trends (Emerson, 1997), which can be indicative of the type of rock being examined. Figure 10(a) shows the full extent of the plot and Figure 10(b) shows only the extent of the data.

Apparent porosity values for this data set are relatively low, with the majority of the samples show a value of <0.25%. The highest apparent porosity observed was 2.57% for sample 20TR2363.

The majority of the samples plotted between the 'felsic' and 'mafic' line. As expected, gabbro, mafic schist and metabasalt plot near the mafic line (Figure 10b).

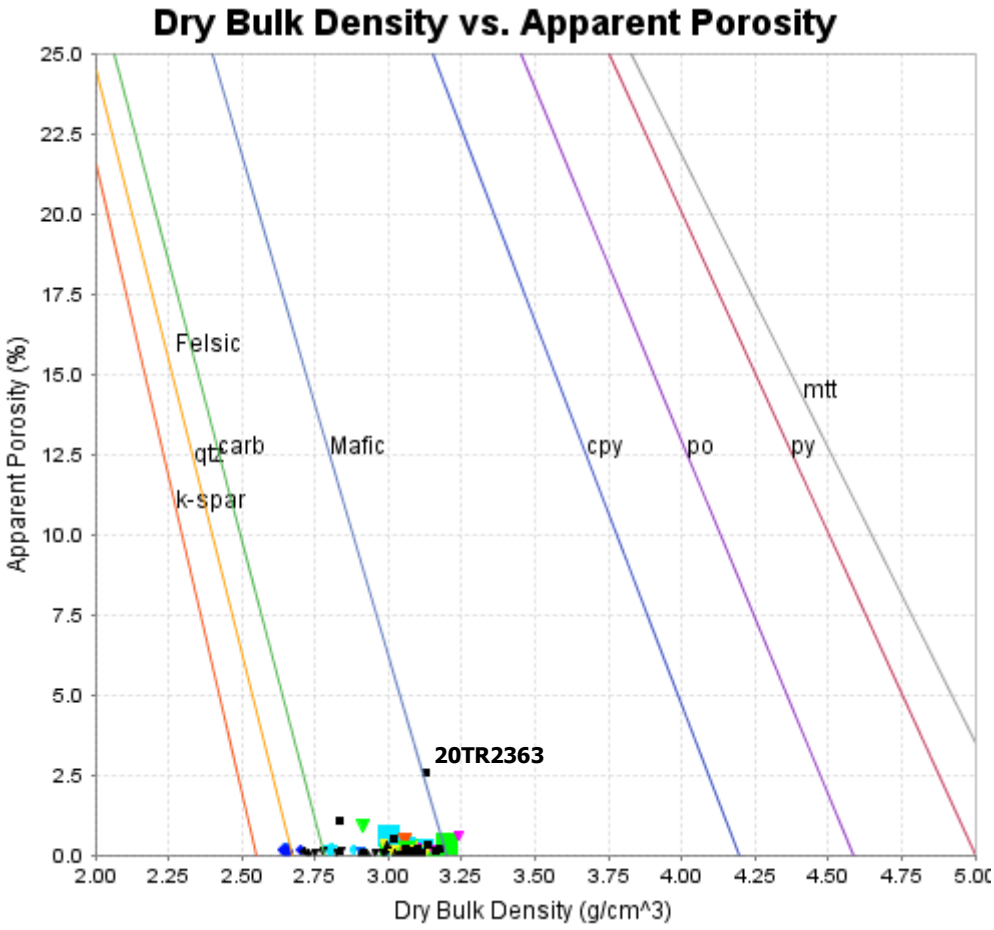

(a)

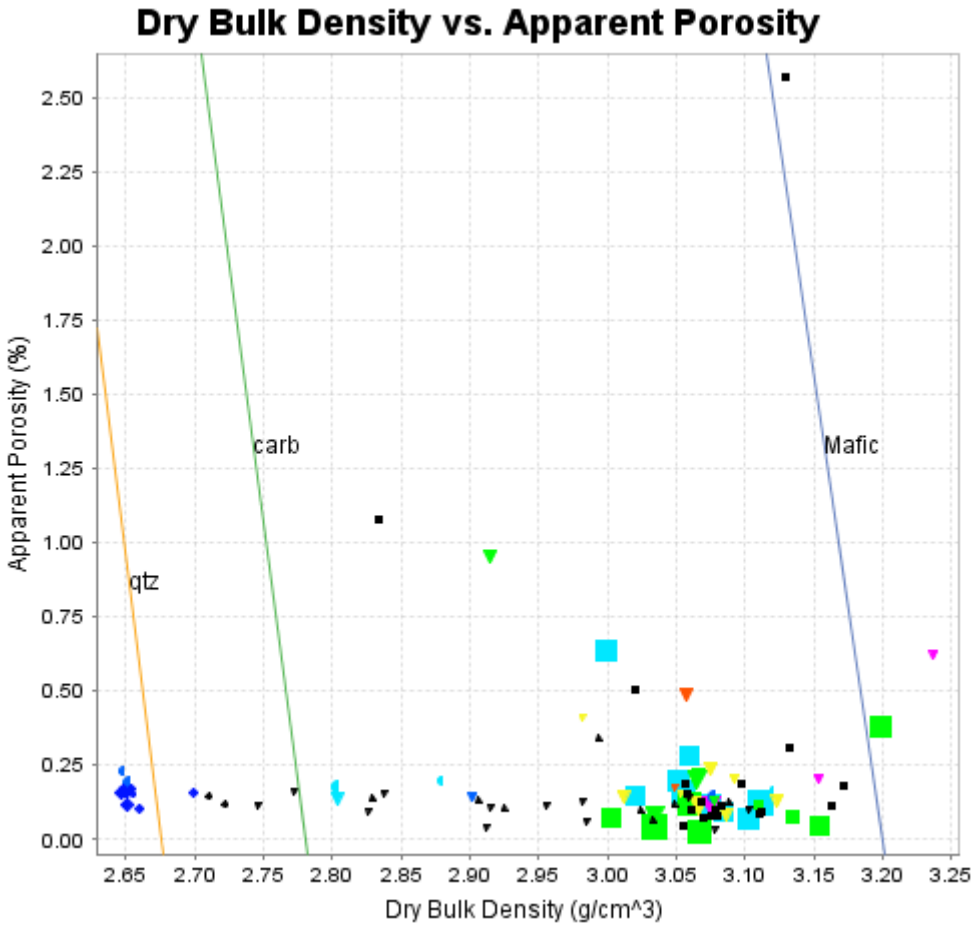

(b)

Figure 10. Cross-plot of dry bulk density against porosity. (a) shows the full extent of the plot, while (b) shows only the extent of the data.

Figure 11 displays dry bulk density plotted against P-wave velocity. Black lines are contours of acoustic impedance with their separation representing the contrast required to produce a minimum reflection coefficient (R=0.06) detectable by the seismic reflection method. The more contours the data overlaps, the more likely the seismic reflection method is to map geological and/or lithological contrasts.

P wave velocity range between 4560 and 6820 m/s, and the data points are spread over multiple contours. From this plot, it can be inferred that seismic reflection may be capable of detecting some contrast between lithologies, particularly felsic vs. mafic.

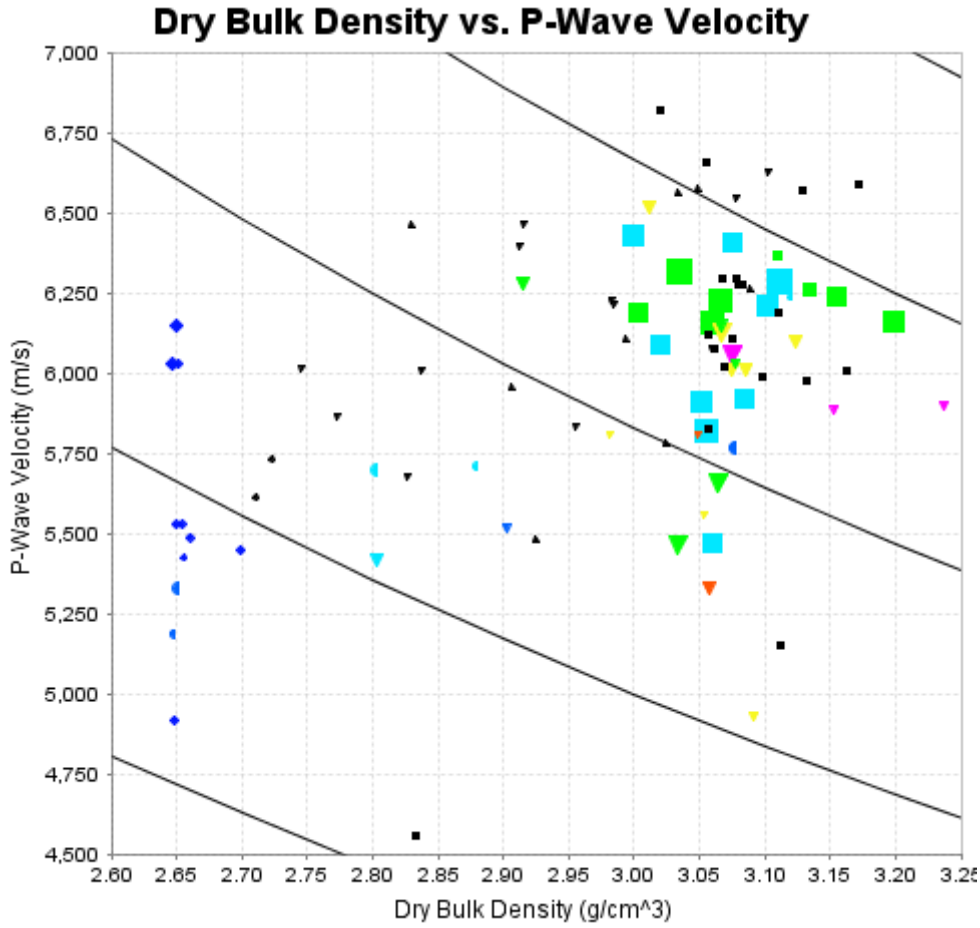

Figure 11. Cross-plot of dry bulk density against sonic (P-wave) velocity.

The induced and remanent magnetic vectors have been measured for samples that exhibited a magnetic susceptibility $>5 \times 10^{-3}$ SI. Measurement samples below this threshold tends to result in noisy, unreliable data. A plot of the intensity of the induced vs. remanent vector intensity (J_{ind} vs. J_{rem}) is shown in Figure 12.

Samples above the dotted line have a remanent magnetisation stronger than an induced magnetisation, i.e. their Koenigsberger Ratio (Q) is >1. Twenty-eight samples were found to be remanent magnetisation dominant, and thirteen were induced-magnetisation dominant (Q<1).

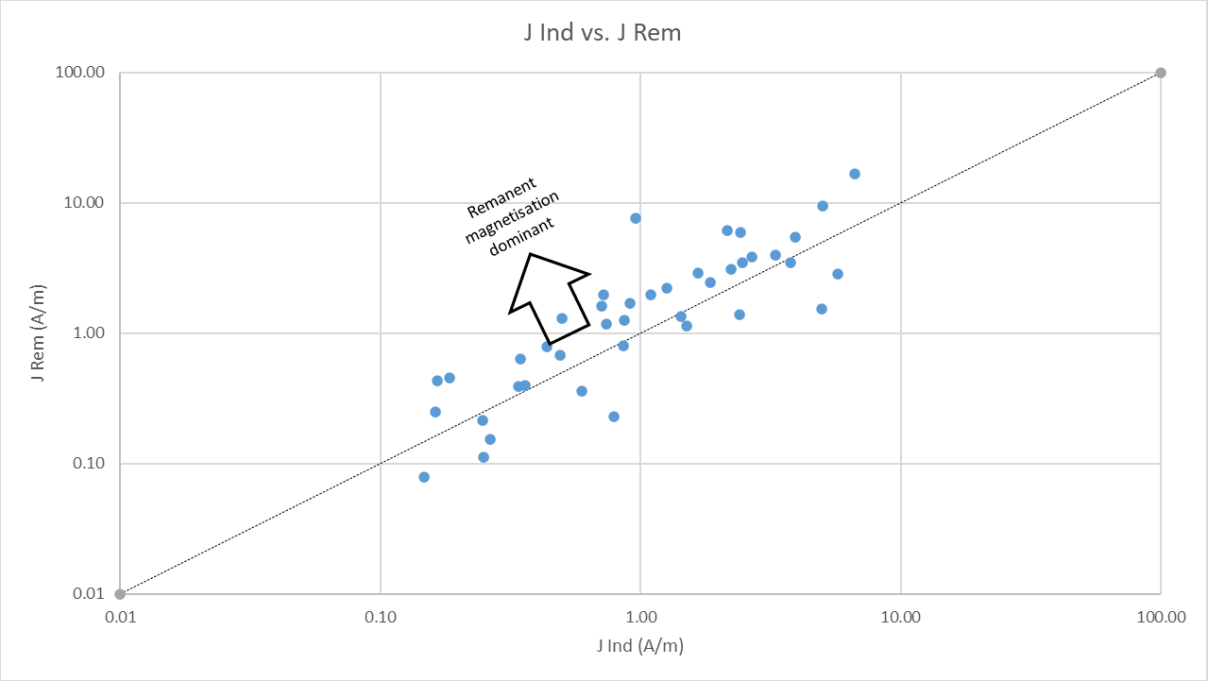

Figure 12. Cross-plot of intensity of J_{ind} versus J_{rem}. Samples above the trend line have Koenigsberger ratio (Q) greater than 1, indicating they are remanent-magnetisation dominant. Conversely, samples below the trend line have a Q value less than one, and are induced-magnetisation dominant.

A magnetic susceptibility value has been calculated from the induced magnetic vector intensity and compared with the measured magnetic susceptibility. A cross-plot of these two values is shown in Figure 13. Induced- and remanent-dominant samples are distinguished by different colours, where grey represents Q<1 and orange represents Q>1.

Samples with similar magnetic susceptibilities derived via each method plot closer to the trend line. Some variation is expected, especially in remanent-dominant (Q>1) samples where the remanent vector can reduce the apparent amplitude of the induced vector via destructive interference. This can be observed especially in samples with a high pyrrhotite content; however, this effect does not appear to be significant in this sample suite.

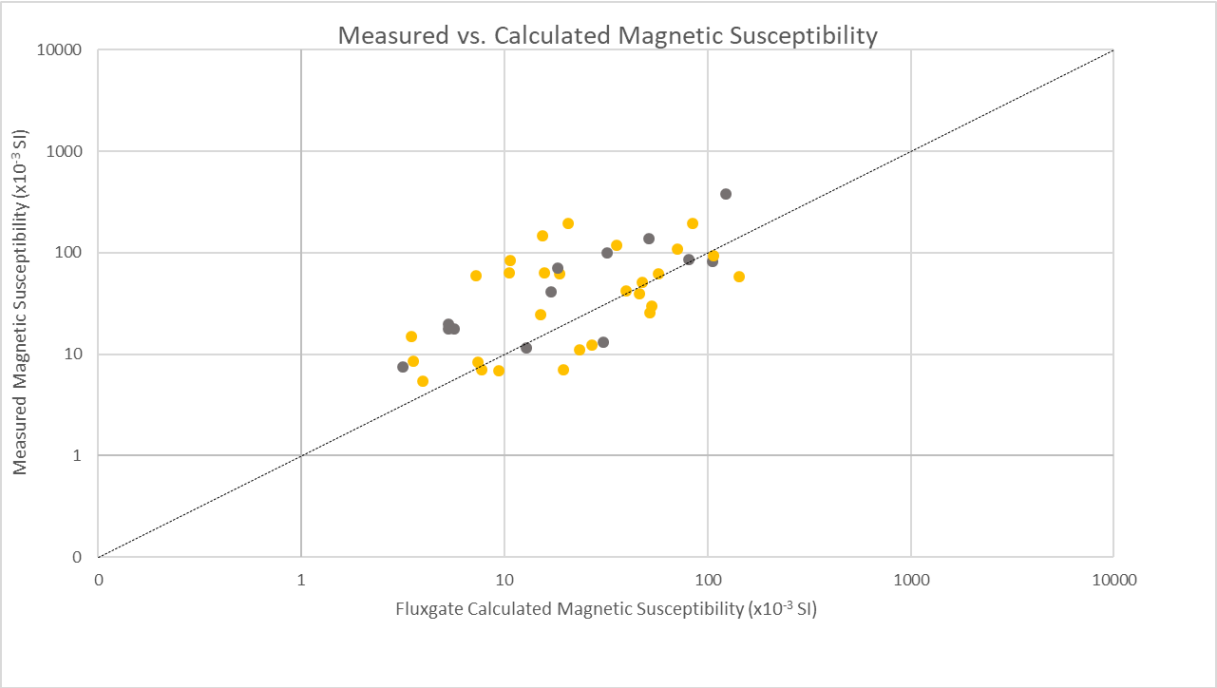

Figure 13. Logarithmic plot of magnetic susceptibility derived from fluxgate against measured magnetic susceptibility.

4. CONCLUSION

Terra Petrophysics has performed petrophysical analysis of 93 rock samples from the Eucla province, Western Australia. Integration of the petrophysical data with geological logging and elemental assays has been performed to aid a better understanding and the potential implications of the physical properties of the data. A summary of the findings is given below.

- There is a strong density contrast between mafic and felsic lithologies. Some variation within each group is observed, and is likely a result of alteration and veining.
- A wide (10^4) range of magnetic susceptibility values is observed in this dataset, however there does not appear to be any significant correlation with other properties, although samples with elevated Ni somewhat correlate with a lower magnetic susceptibility.
- A wide (10^5) range of resistivity values is observed in this dataset. Samples with elevated Ni appear to be less resistive, likely due to the presence of sulphides.
- Most samples showed a chargeability of <50 mV/V, and there were no clear distinctions in the group apart from three unassayed samples of mafic schist/metabasalt that showed very high (>75 mV/V) chargeability.
- All samples in this suite exhibited a weak to nil inductive conductivity response.
- All samples in this suite exhibited a low apparent porosity.
- Based on the sample suite analysed, there may be some merit to seismic reflection as a tool to detect changes in lithology, but more information is needed to draw a firmer conclusion.
- Of the samples that exhibited a magnetic susceptibility >5 $\times 10^{-3}$ SI, 28 were remanent-magnetisation dominant and 13 were induced-magnetisation dominant

5. REFERENCES

Emerson, D.W., 1990, Notes on Mass Properties of Rocks – Density, Porosity, Permeability. Exploration Geophysics, 21, 209-216

Emerson, D.W., and Yang, Y.P. 1997, Insights from laboratory mass property Cross-plots. ASEG Preview, 70, 10-14.

APPENDIX 1 – DATA TABLE

Sample Information					Magnetic Properties		Mass Properties			Seismic Properties		Electrical Properties		
TR Sample ID	Client Sample ID	Drillhole ID	From	To	Magnetic Susceptibility	Koenigsberger Ratio (Q)	Dry Bulk Density	Apparent Porosity	Grain Density	P-Wave Velocity	Acoustic Impedance	Galvanic Resistivity	Chargeability	Inductive Conductivity
			(m)	(m)	(×10^-3 SI)		(g/cm^3)	(%)	(g/cm^3)	(m/s)	(g/cm^3)*(m/s)	(Ωm)	(mV/V)	(S/m)
20TR2286	602643	MAD002	391.30	391.40	0.996		3.12	0.13%	3.13	6100	19053	5182	4.7	0
20TR2287	602644	MAD002	395.43	395.52	1.324		3.08	0.04%	3.08	6550	20161	4927	3.6	0
20TR2288	602645	MAD002	404.15	404.20	81.437	0.32	2.91	0.95%	2.94	6280	18304	70137	9.7	0
20TR2289	602646	MAD002	410.08	410.14	41.261	1.32	2.77	0.16%	2.78	5870	16272	35245	8.2	0
20TR2290	602647	MAD002	412.92	412.98	190.094	11.55	2.80	0.14%	2.81	5420	15194	69565	18.3	0
20TR2291	602648	MAD002	419.59	419.69	6.953	1.18	3.03	0.08%	3.04	5470	16592	12759	18.5	0
20TR2292	602649	MAD002	423.60	423.70	1.199		2.98	0.41%	2.99	5810	17319	646	9.9	0
20TR2293	602650	MAD002	425.10	425.20	0.835		2.99	0.34%	3.00	6110	18287	844	8.6	0
20TR2294	602651	MAD002	430.06	430.16	2.866		3.07	0.12%	3.07	6130	18795	12650	21.2	0
20TR2295	602652	MAD002	434.48	434.57	2.846		3.09	0.08%	3.09	6010	18545	7686	6.0	0
20TR2296	602653	MAD002	436.69	436.79	1.697		3.01	0.14%	3.02	6520	19634	2707	5.7	0
20TR2297	602654	MAD002	440.27	440.36	0.927		2.84	0.16%	2.84	6010	17049	5568	19.4	0
20TR2298	602655	MAD002	447.78	447.88	1.724		3.06	0.49%	3.07	5330	16294	325	13.6	0
20TR2299	602656	MAD002	452.30	452.40	0.757		2.65	0.12%	2.65	6150	16299	126061	11.4	0
20TR2300	602657	MAD002	457.79	457.89	1.816		3.02	0.10%	3.03	5790	17507	7348	13.0	0
20TR2301	602658	MAD002	458.36	458.46	2.661		2.92	0.11%	2.93	5490	16053	12005	74.3	0
20TR2302	602659	MAD002	460.02	460.12	1.171		2.91	0.11%	2.92	6470	18860	8995	10.2	0
20TR2303	602660	MAD002	467.37	467.47	2.132		3.08	0.13%	3.08	6030	18555	8479	7.5	0
20TR2304	602661	MAD002	467.95	468.55	8.279	1.91	2.83	0.15%	2.83	6470	18301	30112	83.4	0
20TR2305	602662	MAD002	469.58	469.64	4.775		2.65	0.16%	2.65	6030	15984	75489	9.4	0
20TR2306	602663	MAD002	470.28	470.37	1.530		2.65	0.17%	2.66	5530	14674	49744	8.3	0
20TR2307	602664	MAD002	475.02	475.12	0.913		2.98	0.13%	2.99	6230	18576	5698	7.1	0
20TR2308	602665	MAD002	479.58	479.67	2.317		3.24	0.62%	3.26	5900	19098	236	6.1	0
20TR2309	602666	MAD002	481.47	481.51	12.198	1.85	3.15	0.20%	3.16	5890	18572	4637	11.4	0
20TR2310	602667	MAD002	484.80	484.90	4.951		2.70	0.16%	2.70	5450	14711	10050	10.7	0
20TR2311	602668	MAD002	485.90	486.00	1.116		2.65	0.16%	2.66	5430	14413	8150	2.2	0
20TR2312	602669	MAD002	490.15	490.20	17.504	0.53	2.71	0.15%	2.71	5620	15224	17499	13.9	0
20TR2313	602670	MAD002	493.44	493.54	1.974		2.65	0.16%	2.65	5530	14649	17161	2.7	0
20TR2314	602671	MAD002	495.35	495.40	29.141	1.44	3.09	0.13%	3.09	6270	19361	10076	23.3	0
20TR2315	602672	MAD002	502.05	502.15	1.392		3.05	0.12%	3.05	6580	20055	2775	11.7	0
20TR2316	602673	MAD002	502.36	502.43	2.073		3.03	0.07%	3.04	6570	19927	4120	11.2	0
20TR2317	602674	MAD002	505.38	505.43	0.670		2.98	0.06%	2.99	6220	18562	6244	10.5	0
20TR2318	602675	MAD002	508.38	508.49	135.953	0.59	2.95	0.12%	2.96	5840	17257	26530	85.2	0
20TR2319	602676	MAD002	510.25	510.30	40.286	0.33	2.75	0.12%	2.75	6020	16527	92366	15.8	0
20TR2320	602677	MAD002	515.20	515.30	2.591		2.65	0.16%	2.65	6030	15957	27127	3.4	0
20TR2321	602678	MAD002	517.16	517.21	61.493	1.51	2.91	0.14%	2.91	5960	17318	50016	24.3	0
20TR2322	602679	MAD002	521.08	521.18	0.982		3.09	0.20%	3.10	4930	15242	1549	11.6	0
20TR2323	602680	MAD002	525.84	525.93	1.425		3.05	0.16%	3.06	5560	16976	1884	9.6	0

Sample Information					Magnetic Properties		Mass Properties			Seismic Properties		Electrical Properties		
TR Sample ID	Client Sample ID	Drillhole ID	From	To	Magnetic Susceptibility	Koenigsberger Ratio (Q)	Dry Bulk Density	Apparent Porosity	Grain Density	P-Wave Velocity	Acoustic Impedance	Galvanic Resistivity	Chargeability	Inductive Conductivity
			(m)	(m)	(×10^-3 SI)		(g/cm^3)	(%)	(g/cm^3)	(m/s)	(g/cm^3)*(m/s)	(Ωm)	(mV/V)	(S/m)
20TR2324	602681	MAD002	530.20	530.30	0.838		3.10	0.10%	3.11	6630	20566	1202	10.4	0
20TR2325	602682	MAD002	535.21	535.30	1.256		3.06	0.14%	3.06	6080	18597	696	7.0	0
20TR2326	602683	MAD002	540.27	540.37	2.145		2.91	0.05%	2.91	6400	18634	8802	6.4	0
20TR2327	602684	MAD002	547.33	547.43	0.981		3.05	0.18%	3.05	5810	17710	737	9.5	0
20TR2328	602685	MAD002	554.75	554.85	1.608		3.07	0.12%	3.08	6060	18634	1335	11.1	0
20TR2329	602686	MAD002	560.68	560.78	1.350		3.08	0.24%	3.08	6010	18482	990	10.0	0
20TR2330	602687	MAD002	565.00	565.11	0.360		2.83	0.10%	2.83	5680	16052	3698	9.0	3.1
20TR2331	602688	MAD002	569.07	569.17	3.361		2.66	0.10%	2.66	5490	14604	43147	6.7	0
20TR2332	602689	MAD002	572.06	572.16	2.623		2.65	0.17%	2.65	4920	13029	21212	6.1	0
20TR2333	602690	MAD002	575.02	575.08	19.444	0.48	2.72	0.12%	2.72	5740	15620	3690	8.8	0
20TR2334	602691	MAD002	580.90	580.96	372.290	0.50	2.90	0.14%	2.91	5520	16019	384067	30.0	0
20TR2335	602692	MAD002	586.83	586.89	7.318	0.53	3.06	0.20%	3.07	5660	17344	3996	7.3	0
20TR2336	602693	MAD002	591.18	591.28	1.101		3.07	0.22%	3.07	6150	18857	1965	3.0	0
20TR2337	602694	HDDH002	315.36	315.41	14.789	1.58	3.08	0.10%	3.08	6300	19390	80609	18.6	0
20TR2338	602695	HDDH002	316.00	316.05	62.986	1.42	3.06	0.15%	3.06	6120	18710	124321	23.7	0
20TR2339	602696	HDDH002	319.45	319.50	98.379	0.76	3.06	0.16%	3.06	5820	17784	13439	17.7	0
20TR2340	602697	HDDH002	325.45	325.49	17.458	0.86	3.06	0.18%	3.06	5830	17817	10113	10.9	0
20TR2341	602698	HDDH002	330.90	330.95	116.007	1.74	3.05	0.20%	3.06	5910	18031	535088	38.6	0
20TR2342	602699	HDDH002	333.35	333.45	3.025		2.65	0.19%	2.65	5330	14122	34304	13.6	0
20TR2343	602700	HDDH002	340.09	340.15	144.306	2.98	3.08	0.14%	3.08	5770	17743	56698	28.6	0
20TR2344	602701	HDDH002	340.46	340.50	82.351	2.64	3.06	0.28%	3.07	5470	16734	19499	17.2	0
20TR2345	602702	HDDH002	342.25	342.30	91.549	2.11	3.08	0.12%	3.09	6280	19362	9613	31.4	0
20TR2346	602703	HDDH002	350.00	350.10	5.324	2.59	3.11	0.09%	3.11	6190	19254	4138329	35.7	0
20TR2347	602704	HDDH002	355.00	355.05	1.249		3.05	0.05%	3.06	6660	20344	3667444	24.7	0
20TR2348	602705	HDDH002	357.00	357.10	0.436		3.06	0.12%	3.06	6160	18850	2142026	34.3	0
20TR2349	602706	HDDH002	360.05	360.10	1.387		3.08	0.08%	3.08	6110	18788	767939	29.8	0
20TR2350	602707	HDDH002	366.81	366.90	3.567		3.10	0.07%	3.10	6210	19262	1452817	20.0	0
20TR2351	602708	HDDH002	372.86	372.93	1.814		3.07	0.07%	3.07	6020	18476	252897	17.9	0
20TR2352	602709	HDDH002	374.80	374.90	1.467		3.00	0.07%	3.00	6190	18586	2357922	26.8	0
20TR2353	602710	HDDH002	379.67	379.73	59.190	1.16	3.03	0.04%	3.04	6320	19175	1014070	22.0	0
20TR2354	602711	HDDH002	381.00	381.06	63.180	1.64	3.10	0.19%	3.10	5990	18556	13781	11.6	0
20TR2355	602712	HDDH002	383.61	383.67	70.387	0.94	3.11	0.13%	3.11	6290	19568	106961	27.9	0
20TR2356	602713	HDDH002	385.00	385.09	8.418	2.97	3.16	0.12%	3.17	6010	19007	36947	24.3	0
20TR2357	602714	HDDH002	391.16	391.25	0.000		2.65	0.23%	2.65	5190	13733	39555	13.8	0.2
20TR2358	602715	HDDH002	392.78	392.86	2.570		3.15	0.05%	3.16	6240	19686	283741	20.7	0
20TR2359	602716	HDDH002	395.00	395.10	10.888	1.84	3.17	0.18%	3.18	6590	20902	6531	11.0	0
20TR2360	602717	HDDH002	401.12	401.18	12.878	0.87	3.20	0.38%	3.21	6160	19702	10920	13.6	0
20TR2361	602718	HDDH002	404.70	404.80	2.407		3.08	0.09%	3.09	5920	18255	1559300	20.4	0
20TR2362	602719	HDDH002	407.00	407.10	4.225		3.07	0.03%	3.07	6230	19104	1011856	25.6	0

Sample Information					Magnetic Properties		Mass Properties			Seismic Properties		Electrical Properties		
TR Sample ID	Client Sample ID	Drillhole ID	From	To	Magnetic Susceptibility	Koenigsberger Ratio (Q)	Dry Bulk Density	Apparent Porosity	Grain Density	P-Wave Velocity	Acoustic Impedance	Galvanic Resistivity	Chargeability	Inductive Conductivity
			(m)	(m)	(×10^-3 SI)		(g/cm^3)	(%)	(g/cm^3)	(m/s)	(g/cm^3)*(m/s)	(Ωm)	(mV/V)	(S/m)
20TR2363	602720	HDDH002	410.00	410.06	57.954	2.56	3.13	2.57%	3.21	6570	20556	10315	24.6	0
20TR2364	602721	HDDH002	415.03	415.13	0.603		3.13	0.31%	3.14	5980	18730	2747	9.3	0
20TR2365	602722	HDDH002	416.77	416.82	38.548	3.27	3.11	0.12%	3.11	6370	19807	53608	9.0	0
20TR2366	602723	HDDH002	422.44	422.54	24.192	2.34	3.13	0.08%	3.14	6260	19619	13574	4.4	0
20TR2367	602724	HDDH002	425.00	425.10	0.744		3.12	0.17%	3.12	6240	19463	81225	10.4	0.1
20TR2368	602725	HDDH002	430.41	430.50	0.890		2.83	1.08%	2.86	4560	12921	459	9.6	0
20TR2369	602726	HDDH002	435.00	435.07	3.831		2.88	0.20%	2.88	5710	16433	2854	5.1	0
20TR2370	602727	HDDH002	440.22	440.28	11.490	0.61	3.11	0.09%	3.12	5150	16028	15682	6.4	0
20TR2371	602728	HDDH002	442.28	442.34	25.489	2.67	2.80	0.18%	2.81	5700	15968	4791	7.6	0
20TR2372	602729	HDDH002	444.45	444.50	61.876	1.47	3.06	0.10%	3.06	6080	18612	12459	14.0	0
20TR2373	602730	HDDH002	450.04	450.10	6.948	1.89	3.08	0.08%	3.08	6280	19342	48980	12.6	0
20TR2374	602731	HDDH002	455.03	455.09	6.732	1.89	3.07	0.13%	3.07	6300	19327	13116	9.3	0
20TR2375	602732	HDDH002	459.35	459.40	190.163	1.43	3.00	0.63%	3.02	6430	19287	2832	11.0	0
20TR2376	602733	HDDH002	466.35	466.40	85.019	0.93	3.07	0.12%	3.08	6410	19711	768096	38.7	0
20TR2377	602734	HDDH002	470.04	470.10	50.328	1.41	3.02	0.50%	3.03	6820	20592	369480	37.6	0
20TR2378	602735	HDDH002	474.30	474.35	106.731	1.25	3.02	0.14%	3.02	6090	18392	717679	56.1	0

APPENDIX 2 – SAMPLE PHOTOS

See attached APPENDIX 2 – Sample Photos.

Markoski et al.

REGIONAL PETROPHYSICS: EUCLA BASEMENT 2020–21

In 2020–21, the Geological Survey of Western Australia (GSWA) commenced a pilot petrophysics project, in collaboration with Terra Petrophysics, and funded by the Exploration Incentive Scheme (EIS). During this project, a suite of physical property measurements were made on EIS co-funded drillcore, stratigraphic drillcore and company drillcore from the Paterson Orogen, West Arunta, Eucla basement and the Kalgoorlie and Yamarna Terranes of the Eastern Goldfields Superterrane. The aim of this project is to provide a petrophysical dataset that can be used to assist with the planning and interpretation of geophysical data, including characterizing the physical property response of stratigraphic units, alteration and mineralization styles, and constraining geophysical models of the subsurface. This Report, produced by Terra Petrophysics, provides a description of the methods used and a first-pass analysis of the petrophysical data acquired in Eucla in 2020–21.

Further details of geoscience products are available from:

Information Centre
Department of Mines, Industry Regulation and Safety
100 Plain Street
EAST PERTH WA 6004
Phone: (08) 9222 3459 Email: publications@dmirs.wa.gov.au

www.dmirs.wa.gov.au/GSWApublications

REPORT 218